Application of laser simulation method for the analysis of crater formation experiment on PALS laser

S. Borodziuk, A. Kasperczuk, T. Pisarczyk

Institute of Plasma Physics and Laser Microfusion,
23 Hery St., 00-908 Warsaw 49, Poland

K. Rohlena, J. Ullschmied

Joint Research Laboratory PALS of the Institute of Physics and Institute of Plasma
Physics, Acad. Sci. CR, Za Slovankou 3, 182 21 Praha 8, Czech Republic

M. Kalal, J. Limpouch

Faculty of Nuclear Sciences and Physical Engineering, Czech Technical University
in Prague, Brehova 7, 115 19 Praha 1, Czech Republic

P. Pisarczyk

Institute of Computer Science, Warsaw University of Technology,
15/19 Nowowiejska St. 00-665 Warsaw, Poland

The crater formation process is studied in the "laser – Al solid target" interactions on the PALS iodine laser facility. A great variety of laser beam parameters are used to irradiate massive aluminium targets. Large laser energies available (up to 600 J) open a possibility to investigate the process of crater formation for physical conditions different from the earlier studies for the lower laser energies. Comparison with the earlier results is presented.

A simple theory, LSM (laser simulation method), has been applied for the analysis of the experimental results. This model leads to a universal relation (scaling law) for the crater relative volume. Our work extends the study of crater formation to the "virtual" macroparticle velocities exceeding $100 \, \text{km/s}$. The scaling law is derived here for this previously unexplored region. An alternative method of studying crater formation is also proposed.

1   Introduction

The investigations of laser interaction with solid targets, and related phenomena, may be already regarded classical plasma physics study. One of the most evident effects appearing in the "laser–target" experiment is the crater formation in solid targets.

The craters can provide some very useful data explaining many interesting features of such experiments. Studying the volumes and shapes of craters produced in an experiment with fixed parameters of laser pulse (energy, pulse duration, focal spot diameter and intensity distribution of target irradiation), target material (type and density), and applying a proper theoretical model, can lead to certain scaling laws. Such laws provide information about the transfer efficiency of the absorbed laser energy into the shock wave propagating in target (is it a hydrodynamic regime?), about laser light absorption efficiency (is it a collisional absorption?), about thermal conductivity, about "quality" (uniformity) of the laser beam, and so on.

It is also very important that the methods of measurement of crater parameters are fairly simple and the crater analysis may be delayed to a suitable time, as the crater remains unchanged for a long time after the experiment.

It has been proved that there is a direct analogy between the cases when a material macroparticle impacts with a high velocity onto a solid target, and the case when a powerful laser pulse irradiates a similar target. The craters arising in massive targets irradiated by laser light may be regarded as a class of so called "high velocity impact" (HVI) problems. It may be treated as a purely scientific problem or it can be applied to certain practical (e.g. industrial) aspects. The laser simulation method (LSM) has been developed [1] to investigate the HVI problems by means of laser–target interaction. Several years ago, this method was successfully applied in the international program of Halley's Comet investigations carried out during its approach to the Sun [2–4]. LSM was used since there was practically no possibility to apply the direct method of HVI using e.g. some macroparticles accelerated to velocities of (60–80) km/s, which was required to investigate the problem of impact of comet dust particles against cosmic probe shield. However, the analogy between HVI and laser produced craters, found at lower impact velocities and the derived scaling laws enable simulation of HVI using laser–target interaction.

At present, we have the opportunity to extend the range of HVI investigations to very high laser intensities, close to 10^{16} W/cm^2, by means of the high power Prague Asterix Laser System (PALS) and to verify the previous results. Our experimental and theoretical studies of crater formation may be also useful in explaining many physical effects and especially those connected with the shock wave propagation. In general, they can help to evaluate certain plasma parameters in the laser interactions with solid targets (e.g. [5,6]) in a simple way.

In the present work we exploit the results of experiments performed on the PALS iodine laser facility. By using LSM certain scaling laws are derived for craters produced in Al targets for various parameters of the laser pulse. Varying laser energy and intensity we scan a broad range of "virtual" macroparticles with velocities exceeding 100 km/s. These equivalent velocities are much higher in comparison with the previous experiments ($v \leq 50$ km/s in Refs. [2,4]). Certain suggestions for next experimental steps will be pointed out.

2   Experimental set-up

The experiment was carried out with the use of the PALS facility. Plasma was generated by an iodine laser beam on the surface of a planar solid target, made of aluminium, by means of an aspherical lens with a focal length of 593 mm. Two harmonics of laser radiation, the first one with the wavelength of $\lambda_1 \approx 1.315\,\mu m$ and the third one with $\lambda_3 \approx 0.438\,\mu m$, were used. The essential investigation was carried out with laser energy of $E_L \approx 100$ J, and pulse duration of 0.4 ns. Additionally, some shots were performed at energy of $E_L \approx 600$ J.
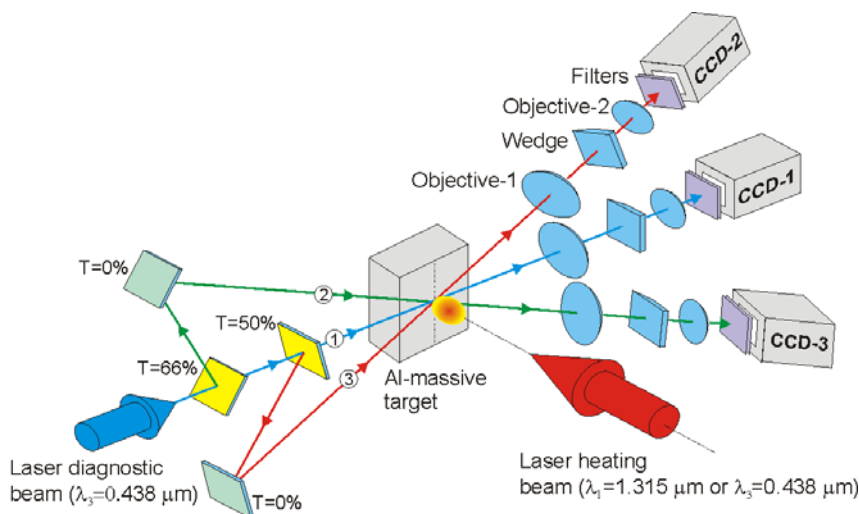

Fig. 1. Scheme of the three-channel interferometric diagnostics.

A three-frame interferometric system with automated image processing was used to study the plasma expansion. The scheme of the three-channel interferometric diagnostics is presented in Fig. 1. The diagnostic system was illuminated by the third harmonic of the iodine laser. The delay between the frames was 3 ns, so that the interferometric measurement during a single shot covered a period of 6 ns only. In order to probe later stages of the plasma expansion, the period of observation in some shots was delayed by 6 ns. Due to a high reproducibility of the plasma expansion at different laser shots, interferogram sequences from different shots may be sewed together. Thanks to that, our observation period was extended up to 12 ns, starting from 3 ns after the maximum of the heating laser pulse. This initial moment actually corresponds to the beginning of the crater formation process [7].

The investigations were carried out at various intensity levels of the laser radiation impinging on the target. These intensities were scaled by changing the focusing lens position. The maximum of the intensity occurring in the focal point corresponded to a minimum focal spot radius of 35 μm.

3   Results and analysis of the crater formation
in iodine laser − Al target interactions

Experimental results of the crater investigation are presented in Fig. 2. The crater dimensions were obtained by means of optical microscopy measurements. In order to obtain the shape of the craters, craters replicas were made of wax.

The characteristic features of craters created in our experiment are as follows. The biggest crater has been produced in the experiment with the highest laser energy ($E_L = 600$ J). Most of the craters (except two) have regular shapes ($\approx$ hemisphere). Two of them resemble rings. For the same laser pulse energies ($E_L = 100$ J), the craters created in experiment with a shorter laser wavelength (λ_3) are apparently larger, compared to those produced by λ_1 radiation.
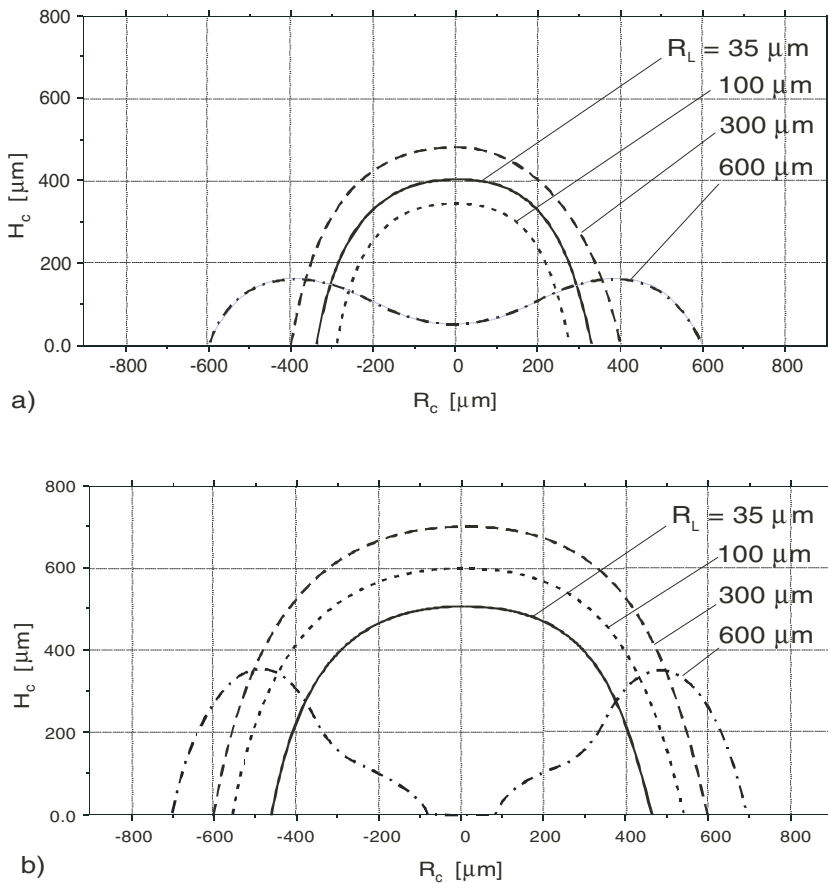

Fig. 2. Crater shapes and dimensions determined on the basis of wax crater replicas, for the first (a) and the third (b) harmonic of the heating laser beam.

What is the reason for the two different crater shapes? We suppose that it is due to the non-uniformity of target irradiation. The output laser beam has a large diameter, equal to several tens cm. Due to it all the optical elements along the beam path to the experimental chamber can cut off the outer parts of the beam. This process results in a diffraction of the laser beam and disturbs the radiation intensity distribution on the target surface. These disturbances are more pronounced when the target position does not coincide with the focal point. Thus, the influence of disturbances is very clearly seen for the maximum focal radius ($R_L = 600\,\mu$m).

To determine the electron density distribution on the basis of the phase shift, special numerical methods have been elaborated [8]. In the case of axial symmetry of the plasma, the relation between the phase of the probing beam and the electron density in a selected cross-section z of the plasma is expressed by the well-known Abel integral equation:

$$S(y) = 2 \int_y^1 \frac{f(r)r}{\sqrt{r^2 - y^2}} \mathrm{d}r, \qquad (1)$$

where $f(r) = 4.46 \times 10^{-14} \lambda R n_e(r)$, y and r are the dimensionless coordinates (normalized by R) corresponding to one another in an interferogram plane and a real plasma cross-section, respectively, $S(y)$ is the phase distribution [rad/2π], $n_e(r)$ – electron density distribution [cm^{-3}], λ – wavelength of laser radiation [cm], and R – radius of plasma for the selected cross-section [cm].

Having full information about the electron density distribution, $n_e(r, z)$, calculation of a total electron number could be carried out by numerical integration.

Interferometric measurements allowed us to observe the process of the outflow of plasma from the crater. The essential information about this process is presented in Figs. 3 and 4. Figure 3 illustrates the outflow of plasma from the crater for the two wavelengths used. Here the plasma stream borders are represented by equidensity line of $n_e = 2 \times 10^{17}$ cm^{-3}. The second equidensity line corresponds to $n_e = 3 \times 10^{18}$ cm^{-3} and all other equidensity lines are separated by $n_e = 3 \times 10^{18}$ cm^{-3}.

With the shorter wavelength, the plasma blob has dimensions approximately twice as large as that created by the longer one. The more intensive outflow of plasma results in a bigger crater. The diagrams presented in Fig. 4 show the changes of total electron number as a function of time, for the same two cases. In the case of the longer wavelength, the outflow of plasma has approximately a uniform character (the total electron number is roughly conserved at a level of 2×10^{16}), while for the shorter wavelength the total electron number grows very fast with time, reaching the value of about 8×10^{16} at time $\Delta t = 15$ ns. Thus, such diagrams can provide information on the dynamics of the crater creation process.

In other words, one may conclude that a shorter laser wavelength means deeper laser penetration (higher critical density), and more efficient collisional absorption. Consequently, the laser-induced shock wave is stronger, and the mass of the material ejected from the target and the crater volume are enhanced.

The experimental results show that the optimum focal beam radius is $300\,\mu$m. It provides the biggest crater volumes for both laser wavelengths. This is a fairly large
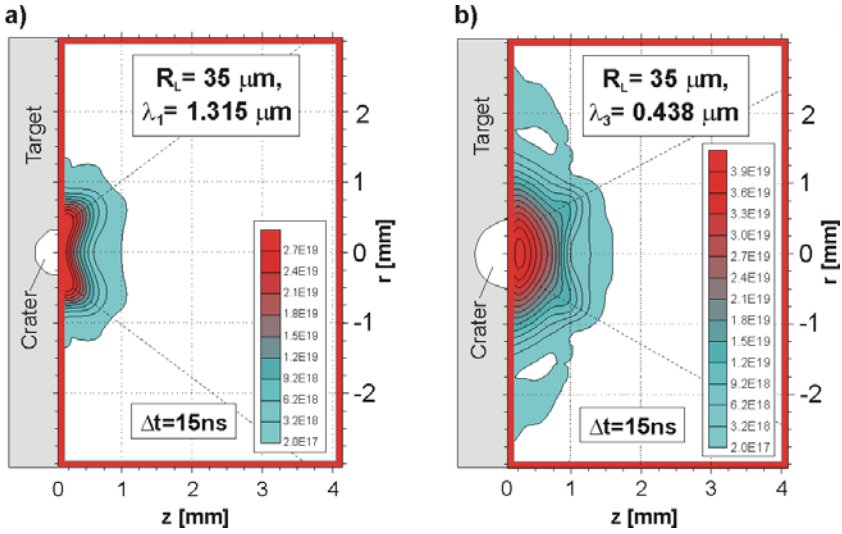
Fig. 3. Electron density (cm^{-3}) in the plasma outflows from the craters for laser spot radius $R_L = 35\,\mu\text{m}$ and delay $\Delta t = 15\,\text{ns}$ at two different wavelengths: a) $\lambda_1 = 1.315\,\mu\text{m}$, b) $\lambda_3 = 0.438\,\mu\text{m}$. The oblique dotted lines denote an approximate boundary of the outflow from the crater.
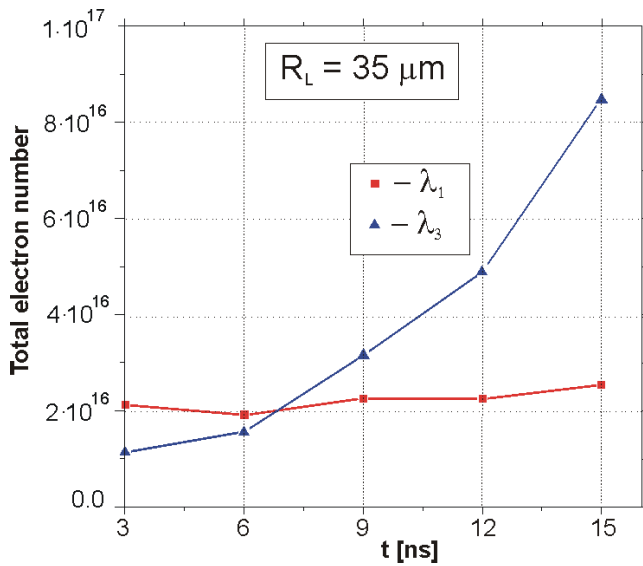

Fig. 4. Total electron number in the plasma outflow versus time delay after laser pulse maximum.

focal spot. However, the laser intensity $I_L \approx 10^{14}\,\mathrm{W/cm^2}$ is capable to generate a strong axial shock wave. The absorption is efficient ($\approx$ 50–60%), the lateral heat conduction can be relatively small, and there is no problem with fast electron generation. For smaller values of R_L (it means that the laser light intensity is higher) all these undesirable effects are stronger (especially for longer laser wavelength $\lambda_L = 1.315\,\mu\mathrm{m}$), and the transfer of the absorbed laser energy into the shock wave is less efficient. So, why not also for the $R_L = 600\,\mu\mathrm{m}$? We suppose that the problem consists in the above mentioned non-uniformity of the laser beam.

The problem of crater formation in laser – solid target interaction may be treated by means of the laser simulation method (LSM). A laser beam, similarly to a macroparticle moving with a high velocity, transmits a considerable part of its energy and momentum to a solid target. As a result, a shock wave is generated. At proper laser intensity ($\geq 10^{13}\,\mathrm{W/cm^2}$) it can achieve a velocity of the order of several km/s and a pressure of the order of megabars. A violent evaporation of the target material takes place, and a crater appears in the spot, where laser radiation illuminates the target. The crater size depends on the focal spot diameter, intensity and duration of the laser pulse. The crater created by a macroparticle colliding with the target varies with its size, velocity, and also with the particle and target materials. Thus, there is a close analogy between these two processes. This analogy becomes a basis for simulation models of various types, e.g. [2, 4].

The idea of the laser simulation method [1] is based on the assumption that the effect of irradiation of the target by a laser beam with energy E_L, pulse duration τ_L, and focus diameter D_L, is similar to that of a collision of a target and a projectile of the diameter D_p, thickness L_p and velocity v, provided the pressure, size and interaction time remain equal.

The basic assumptions for such simulation can be defined as follows:
- pressure p_L created at the target by the laser pulse should be equal to the pressure which is created as a result of macroparticle–target collision, i.e., $p_L = p_p$;
- focus diameter of the laser beam should be equal to the diameter of the macroparticle striking the target $D_L = D_p$ and the laser beam spot should be homogeneous one;
- laser pulse duration should be equal to the shock wave propagation time in the macroparticle–target interaction, thus, $\tau_L = \tau_p$.

In order to analyze the problem formulated in such a way, it is useful to employ the following additional relationships [9]:

$$p_p = \rho_p D u, \qquad (2)$$

$$D = a + bu, \qquad (3)$$

where ρ_p, D, and u are macroparticle mass density, shock wave velocity and material velocity, respectively.

Coefficients a and b are determined experimentally for given materials (shock adiabate). Moreover, it can be assumed for strong shock waves (like in our case) that [10]

$$u = \frac{v}{1 + \dfrac{\rho_{\mathrm{p}}}{\rho_{\mathrm{T}}}}, \tag{4}$$

where v is the velocity of the incident macroparticle and ρ_{T} is the target density.

Our experiment is equivalent to the Al impact on Al target, and the above equations may be simplified for the same target and macroparticle materials, as follows:

$$D = a + b\frac{v}{2}, \tag{5}$$

$$p_{\mathrm{p}} = \rho_{\mathrm{p}}\left(a + b\frac{v}{2}\right)\frac{v}{2}. \tag{6}$$

The relationship between the time of interaction ($\tau_{\mathrm{L}} = \tau_{\mathrm{p}}$), the macroparticle length (L_{p}) and velocity (v) can be written in the form [2]

$$p_{\mathrm{L}}\tau_{\mathrm{L}} = \rho_{\mathrm{p}}L_{\mathrm{p}}v. \tag{7}$$

The ablation pressure has to be calculated or alternatively, it can be matched with the experimental data (see e.g. [11]). Aluminum targets were often used in "laser – solid target" experiments and all the needed data on ablation pressure and material constants are well known. Following the procedure of Ref. [4] one can get an explicit formula for v:

$$v = A^{1/2} - \frac{a}{2b}\left[1 + \left(\frac{\rho_{\mathrm{p}}}{\rho_{\mathrm{T}}}\right)^{1/2}\right], \tag{8}$$

where

$$A = \frac{100}{(\rho_{\mathrm{p}}b)}\left[1 + \left(\frac{\rho_{\mathrm{p}}}{\rho_{\mathrm{T}}}\right)^{1/2}\right]p_{\mathrm{L}} + \left[\frac{a}{2b}\left(1 + \left(\frac{\rho_{\mathrm{p}}}{\rho_{\mathrm{T}}}\right)^{1/2}\right)\right]^2 \qquad [\mathrm{p_L\ in\ Mbar}]. \tag{9}$$

We have assumed $\rho_{\mathrm{p}} = \rho_{\mathrm{T}} = 2.7\,\mathrm{g/cm^3}$, $a = 5.3\,\mathrm{km/s}$ and $b = 1.30$ [2].

The next step is to calculate (using Eq. (7)) the length of a simulated macroparticle L_{p}. This method enables us to present the velocity and the size of projectile as a function of the experimental conditions (laser parameters, material of irradiated target) and to determine the proper scaling laws for the laser-created craters.

Table 1 shows the laser-beam characteristics, and the parameters of craters, measured in the "laser – Al target" interactions. The velocity v, and thickness L_{p} of the corresponding "virtual" macroparticle, calculated by means of LSM, are shown as well. The "relative crater volume" K is defined as $K = V_{\mathrm{c}}/V_{\mathrm{p}}$, where V is the volume of material ejected out of the target in which a crater was burnt, and V_{p} is the volume of a macroparticle colliding with the target. The macroparticle of volume V_{p} was taken to be a cylinder of a radius R_{L} and height L_{p}.

The dependence of the relative volume K on the equivalent macroparticle velocity v is demonstrated in Fig. 5 for the analyzed experimental events. The dependence was fitted with the formula $K = \alpha\,v^{\beta}$. The relative volume K velocity

Table 1. Experimental data and the basic parameters of "virtual" macroparticles (v, L_{p}) obtained by means of LSM. R_{L} is the laser spot radius, D_{c} is the crater diameter, H_{c} is the crater depth, I_{L} is the laser intensity, v is the equivalent macroparticle velocity, L_{p} is the macroparticle thickness and K is the crater relative volume.

No.	R_{L} (μm)	D_{c} (μm)	H_{c} (μm)	I_{L} (W/cm^2)	v (km/s)	L_{p} (μm)	K
$\lambda_1 = 1.315\,\mu$m, $E_{\mathrm{L}} = 100$ J							
1	35	660	400	6.5×10^{15}	68.6	19.0	1178.0
2	100	560	340	8.0×10^{14}	35.8	10.4	159.0
3	300	800	480	8.8×10^{13}	17.6	5.5	89.3
4	600	1260	160	2.2×10^{13}	11.3	3.8	29.6
$\lambda_1 = 1.315\,\mu$m, $E_{\mathrm{L}} = 600$ J							
5	600	1600	600	1.3×10^{14}	20.9	6.4	90.7
$\lambda_3 = 0.438\,\mu$m, $E_{\mathrm{L}} = 100$ J							
6	35	950	500	6.5×10^{15}	115.0	31.0	1756.0
7	100	1100	600	8.0×10^{14}	58.9	16.5	655.0
8	300	1200	700	8.8×10^{13}	28.7	8.5	199.0
9	600	1400	280	2.2×10^{13}	18.3	5.6	55.4

dependence is essential, but K depends also on some others parameters (density of the target, shape and density of the projectile etc).

The resulting scaling law determined by means of LSM on the basis of our experimental measurements has the form $K = 0.35v^{1.84}$. The range of the calculated velocities of "virtual" macroparticles spreads from about $10\,\mathrm{km/s}$ to more than $100\,\mathrm{km/s}$ (see Table 1).

We note that a fairly smooth curve is obtained for a wide range of experimental parameters. Laser intensity I_{L} is varied from 2×10^{13} to $6 \times 10^{15}\,\mathrm{W/cm^2}$, and two different laser wavelengths are used. It may prove that the dominant mechanism of the absorbed laser-energy transfer to the solid target is the propagation of a shock wave even in the range of high laser intensities $I_{\mathrm{L}} \approx 10^{15}\,\mathrm{W/cm^2}$ and laser wavelength $\lambda_1 = 1.315\,\mu$m. These values are outside the validity of the rule $I_{\mathrm{L}}\lambda_L^2 \le 10^{14}\,\mathrm{W\mu m^2/cm^2}$ for a hydrodynamic regime of the ablation process. Some other effects like generation of hot electrons, electron thermal conductivity, and thermal radiation, may influence the process of crater formation by carrying away a significant part of the laser energy.

The scaling law for $K(v)$ calculated in our present work is close to those obtained earlier [2, 4]. They are all compared in Fig. 6. By taking into account the accuracy of experimental data, and also some theoretical assumptions made in our calculations, one may say that the results reported in the present work are in a
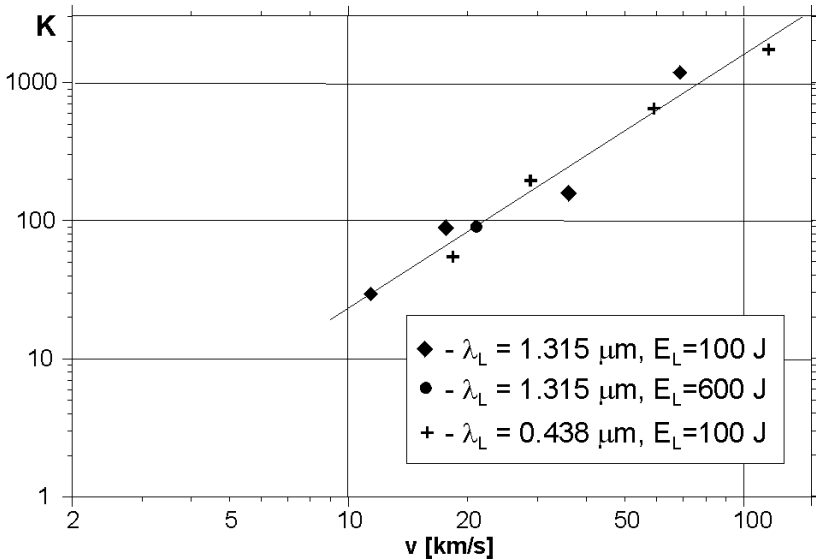
Fig. 5. Dependence of relative crater volume K on the impact velocity v obtained for the data of "iodine laser – Al target" interaction (exact values for all discrete points are taken from Table 1).

good agreement with those acquired earlier. The basic difference is that our experiments were performed for much higher laser energies (and also intensities) and for two different laser wavelengths (λ_1, λ_3) which corresponds to a much wider range of "virtual" macroparticle velocities (up to more than $100\,\mathrm{km/s}$ comparing to $\leq 45\,\mathrm{km/s}$ in Ref. [2]). Extrapolated curves of Refs. [2] and [4] (see Fig. 6) are very close to our present results in the vicinity of $v = 100\,\mathrm{km/s}$. It may be a proof that LSM works well also for higher laser and plasma parameters and it is likely universal in its nature.

LSM is not the only way in which one can study the problem of crater formation in a solid target irradiated by an intense laser beam. The most precise calculations need to use complicated multidimensional hydrodynamic codes, and proper equations of state of the target materials. A much simpler method has been developed in Ref. [5], and applied in Ref. [6] to analyze the problem in terms of, so called, ablating loading efficiency of transfer of the absorbed laser energy into the energy of shock wave. Perhaps, the most natural simulation of the HVI problem by laser methods is to use the collisions of ablatively accelerated thin foils with massive targets. In this case one uses double targets. The massive target is placed at a distance where the accelerated foil fragment has been accelerated to a high velocity and, simultaneously, its density is comparable to the initial solid density. By changing the foil thickness and the laser intensity and, possibly, the distance between the irradiated foil and the massive target, one can get a wide range of projectile velocities. The projectile velocities may have much higher values, than those achieved in LSM.
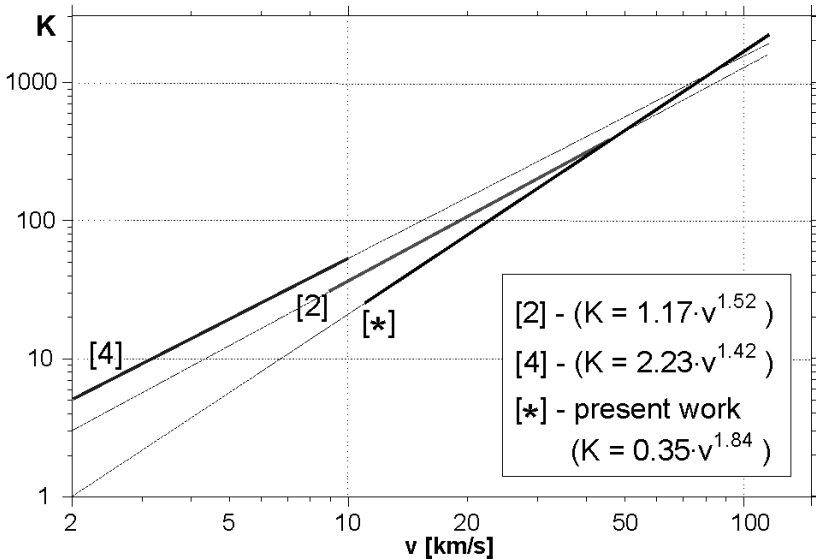
Fig. 6. Comparison of the relative volume K of craters obtained by means of LSM in Refs. [2,4] and in the present measurements.

This method, called "Laser Ablative Acceleration Method" (LAAM) [12], leads to a much broader range of masses and velocities of real projectiles hitting the target. So, a natural step to enter the area of higher projectile velocities is to apply the same iodine laser in the experiment with a double target.

4 Summary

The problem of crater formation was investigated in "iodine laser – Al target" experiment. Laser simulation method (LSM) was applied to study this process as a kind of high-velocity impact (HVI) problems. The scaling law for the relative crater volume K dependence on the velocity v of the "virtual" macroparticle was obtained.

The results of our investigations have been compared with those acquired earlier for lower energies and intensities of Nd lasers. The extrapolated values of $K(v)$ dependence calculated in the past are very close to our present results. Thus, one may conclude that $K(v)$ has a fairly universal nature. The calculated points fit well the curve $K = 0.35\,v^{1.84}$ for a wide range of velocities and for two different laser wavelengths (λ_1 and λ_3 of iodine laser). It may prove the dominance of hydrodynamic nature of the crater formation process, even for high laser intensities of the order of $10^{15}\,\mathrm{W/cm^2}$.

The optimum experimental conditions, which lead to regular, large volume craters, are as follows: a uniform high-intensity short wavelength laser beam, which is efficiently absorbed, and generates a strong axial shock wave. The accompanying

energy loss mechanisms (fast electron generation, lateral heat conduction, thermal radiation) should not play an important role.

How can one verify the applicability of LSM (which seems to be a little bit artificial one)? The best way is to apply the real projectile having the same parameters (V_p, r_p, L_p, D_p, v) as the "virtual" macroparticle assumed in our LSM calculations. So, the next step is to apply double targets (LAAM), which can provide a more precise tool for an investigation of the crater formation process. This is exactly what we are planning to do.

References

[1] A.N. Pirri: Phys. Fluids **20** (1977) 221.

[2] J.P. Bibring, J.P. Bibring, F. Coffet, M. Hallouin, Y. Langevin, and J.P. Romain: J. Physique – Lett. **44** (1983) L-189.

[3] W.M. Burton: Advances in Space Research **2** (1982), issue 12, 255.

[4] S. Borodziuk, S. Denus, J. Farny, J. Kostecki, S. Nagraba, P. Parys, and J. Wołowski: J. Tech. Phys. **28** (1987) 401.

[5] K.S. Gus'kov, S.Yu. Gus'kov: Quantum Electronics **31** (2001) 305.

[6] A.A. Rupasov, E.A. Bolkhovitinov, I.Ya. Doskach, A.A. Erokhin, S.I. Fedotov, L.P. Feoktistov, S.Yu. Gus'kov, B.V. Kruglov, M.V. Osipov, V.N. Puzirev, V.B. Rozanov, A.S. Shikanov, V.B. Studentov, B.L. Vasin, and O.F. Yakushev: *The features of craters formation on the target under the action of powerful laser pulse*, ECLIM 2002, Moscow, October 7–11, 2002, (Ed. S. Zu. Gus'kov), paper Mo-CP/P12, Proc. SPIE, Vol. 5228.

[7] A. Kasperczuk, M. Kalal, B. Kralikova, K. Masek, M. Pfeifer, P. Pisarczyk, T. Pisarczyk, K. Rohlena, J. Skala, and J. Ullschmied: Czech. J. Phys. **51** (2001) 395.

[8] A. Kasperczuk and T. Pisarczyk: Optica Applicata **31** (2001) 63.

[9] Ya.B. Zel'dovich and Yu.P. Raizer: *Physics of Shock Waves and High-Temperature Hydrodynamic Phenomena*, Academic, New York, 1966.

[10] L.V. Al'tshuler: Zh. Eksp. Teor. Fiz. **72** (1977) 317.

[11] R.J. Harrach and A. Szoke: *Shock Waves in Condensed Matter*, A.I.P. Conf. Proc., Vol. 78, 1982, p. 164.

[12] S. Borodziuk and J. Kostecki: Laser Particle Beams **8** (1990) 241.